RESEARCH ARTICLE
doi: 10.2306/scienceasia1513-1874.2026.062

ScienceAsia 52 (3): 2026: ID 2026062: **1–9**

Application of thermally treated granulated attapulgite for advanced treatment of membrane bioreactor effluent

Na Lv[a,*], **Sisi Fan**[a,b]

[a] Lianyungang Technical College, Lianyungang 222000 China
[b] City University of Macau, Macau 999078 China

*Corresponding author, e-mail: lzylvna@163.com

Received 26 Jul 2025, Accepted 8 Jun 2026
Available online 30 Jun 2026

ABSTRACT: Thermally treated granulated attapulgite (TGAT) with increased metal ion content and improved internal structure was employed to further improve the effluent quality of membrane bioreactor (MBR), and its effect on the effluent of anoxic/oxic MBR (A/O-MBR) was investigated. The A/O-MBR fixed-bed column reactors were constructed and filled with unmodified granulated attapulgite (GAT) and TGAT, respectively. Under the conditions of membrane effluent total phosphorus and total nitrogen concentrations of 1.24–2.33 and 14.09–17.55 mg/l, respectively, the fixed-bed column filled with TGAT showed better nitrogen and phosphorus removal effects, with significantly improved effluent quality, when compared with fixed-bed column filled with GAT. Fourier transform infrared spectroscopy and inductively coupled plasma emission spectroscopy proved that the reduction of hydroxyl structure and increase in metal ions in attapulgite after thermal treatment were more conducive to phosphate capture and biofilm formation. TGAT removed nitrogen and phosphorus pollutants from wastewater predominantly through the action of denitrifying microorganisms and precipitation, respectively. Following extended operation of the reactor, elevated nitrogen and phosphorus levels were noted on the surface and within the filler. Application of the used TGAT adsorbent as fertilizer increased plant height, leaf width, fresh weight, and dry weight by 75.13%, 84.64%, 202.48%, and 204.13%, respectively. Thus, TGAT could be used for the advanced treatment of membrane effluent and applied as a slow-release fertilizer to achieve reuse of resources.

KEYWORDS: attapulgite, fixed-bed column, advanced treatment, membrane bioreactor, slow-release fertilizer

INTRODUCTION

Anoxic/oxic membrane bioreactor (A/O-MBR) is an efficient wastewater treatment process, with characteristics of low carbon footprint, high degree of automation, compact arrangement of treatment units, good effluent quality, etc., and has been widely used in domestic wastewater treatment [1]. A significant reduction in pollutant concentration is observed in domestic wastewater treated by A/O-MBR [2]. Zhou et al [3] reported effluent chemical oxygen demand (COD), ammonia nitrogen (NH_4^+-N), total nitrogen (TN), and total phosphorus (TP) concentrations of 32.69, 1.39, 16.47, and 1.60 mg/l, respectively, following A/O-MBR treatment of domestic wastewater. Yuan et al [4] used a multistage A/O-MBR to treat domestic wastewater and attained effluent COD, TN, and TP removal efficiencies of 95%, 85%, and 84%, respectively. Nevertheless, despite the significant reduction in the pollutant concentrations in wastewater treated by A/O-MBR, most of these levels are still higher than the limits specified in the standard (GB18918-2002), thereby requiring advanced treatment.

Addition of chemical removal agents, such as aluminum sulfate, into the biological treatment effluent can achieve substantial removal of pollutants, with TP removal efficiency exceeding 99% [5]. Adsorption phosphorus removal technology has become one of the mainstream methods for advanced treatment of wastewater owing to its advantages, such as low treatment cost, good effluent quality, and sustainable utilization of adsorbents [6, 7]. Moreover, it is imperative to note that natural adsorbents saturated with nitrogen and phosphorus can be used as fertilizers or soil amendments to promote plant growth and achieve recycling of nitration and phosphorus resources in wastewater [8, 9]. Yu et al [10] utilized sludge-derived biochar to recover NH_4^+-N and PO_4^{3-}-P, and applied the adsorbed products as fertilizer. Their pot experiment demonstrated that the adsorbed products could better promote cabbage growth, with the weight of the cabbage being 64.49 g heavier than that of the control. Furthermore, Huang et al [11] prepared a dolomite-alginate composite pellet and investigated the slow-release ability of the material after phosphate adsorption. Their results showed that phosphate in wastewater was adsorbed to the adsorbent surface in the form of calcium phosphate/magnesium phosphate, and that about 90% of phosphate was slowly released into the soil in about 60 days. These saturated phosphate adsorbents can be used as slow-release phosphorus fertilizers to promote agricultural production. Zhao et al [12] prepared an adsorbent composed of two different clays for the treatment of wastewater with high concentrations of NH_4^+-N, which could adsorb 75.5 mg/g nitrogen under static adsorption conditions, and also investigated its potential application as a slow-release fertilizer. Natcha Sornhiran et al [13] re-

covered phosphorus (P) from wastewater using metal-modified biochar and reused it as a phosphate fertilizer. During a 45-day cultivation period, sandy soil samples amended with Al- and Fe-biochar gradually released available P, serving as a long-term P source for plant uptake.

In the present study, granulated attapulgite (GAT) was calcined at high temperatures to obtain thermally treated granulated attapulgite (TGAT) that was applied to enhance the removal of pollutants from domestic wastewater. The physicochemical properties of the modified fillers were characterized by Fourier transform infrared spectroscopy (FTIR) and inductively coupled plasma emission spectroscopy (ICP-OES), and the removal effects of the adsorbent on the pollutants in wastewater were examined. TGAT exhibited good pollutant removal efficiency and adsorption properties and was noted to be safe and environment-friendly. To further investigate the efficacy of TGAT in removing pollutants when used in combination with A/O-MBR from low-concentration wastewater as well as determine the ability of TGAT to achieve standard discharge parameters for domestic wastewater, an A/O-MBR fixed-bed column reactor was established and the effects of TGAT on removing nitrogen (N) pollutants (NH_4^+-N, NO_x-N, TN) and P pollutants were investigated. In addition, the potential use of the saturated adsorbent as crop fertilizer was also discussed. The results obtained provided valuable reference for the practical application of the new adsorbent as well as for the sustainable utilization of N and P resources in wastewater for agricultural purposes.

MATERIALS AND METHODS

Materials

Table 1 The concentration of major pollutants in wastewater.

Water quality index	Concentration (mg/l)
COD	155 ± 16
BOD_5/COD	0.63
NH_4^+-N	28.3 ± 2.0
NO_3^-N	0.28 ± 0.05
TN	30.5 ± 1.2
TP	3.09 ± 0.30
pH	7.1 ± 0.4

The GAT was purchased from Dingbang Mineral Products Technology Co., Ltd., Changzhou City, Jiangsu Province, China, with a particle size of 0.5–1.0 mm. All the chemical reagents used were of analytical grade and purchased from Shanghai Maclin Biochemical Technology Co., Ltd., Shanghai, China. The activated sludge and wastewater used were obtained from a wastewater treatment plant in Lianyungang, Jiangsu, China. The water used was synthetic domestic wastewater, and the water quality indices are summarized in Table 1.

Preparation of TGAT

To obtain TGAT, the GAT was washed thrice with deionized water to remove surface impurities and calcined at 700 °C [14] for 12 h using a muffle furnace to improve its pollutant removal capacity.

Structural parameters of the experimental device

The A/O-MBR fixed-bed column reactor was fabricated from plexiglass. The dimensions of the anoxic tank and the aerobic tank are $20.0 \times 20.0 \times 18.0$ cm, with an effective working dimensions of $20.0 \times 20.0 \times 15.0$ cm. Polyvinylidene fluoride (PVDF) was adopted as the membrane material. The membrane module, with an effective filtration area of 0.0408 m^2, was submerged in the aerobic tank. An aeration device was installed beneath the membrane module to provide oxygen supply and membrane surface scouring. The membrane module was connected to a peristaltic pump through a silicone tube. The pump rotating speed was regulated to maintain a constant membrane flux of 19.33 l/(m^2 h). The reflux ratio was set at 4:1, and the operating temperature is controlled at 25 ± 1 °C. The A/O-MBR effluent was utilized as the influent of the fixed-bed column. The structural parameters of the fixed-bed column are shown in Table 2. The column filled with GAT up to 30-cm height was marked as the C-column (control), while that filled with TGAT was labelled as the T-column.

Table 2 Fixed-bed structure parameters.

Fixed-bed parameter	Value
Diameter	5 cm
Cross-sectional area	19.63 cm^2
Inlet velocity	8.5 ml/min
Bed height	30 cm
The amount of adsorbent filling	350.24 g

Analysis

A Quantachrome QUADRASORB SI (Quantachrome Instruments, Boynton Beach, Florida, USA) specific surface area analyzer was used to determine the surface area and pore volume of GAT and TGAT. A Perkin Elmer 8300 (PerkinElmer Inc., Waltham, Massachusetts, USA) ICP-OES was employed to quantitatively analyze the metal elements in TGAT. The surface morphology of the adsorbent was examined by using a Hitachi S4800 scanning electron microscope (SEM, Hitachi High-Technologies Corporation, Tokyo, Japan). The Zeta potential of the adsorbent before and after modification was measured with a Malvern Zetasizer Nano ZS90 Zeta instrument (Malvern Panalytical Ltd., Malvern, Worcestershire, UK). A Perkin-Elmer Spectrum GX FTIR (PerkinElmer Inc., Waltham, Massachusetts, USA) was used for the surface functional group analysis of the samples.

The potential application of used TGAT adsorbent as a crop fertilizer was investigated by pot experiment. In brief, TGAT was mixed with soil at a ratio of 1:20 and cured in the greenhouse for a week to study the effects of TGAT on the growth of rape (control group was incorporated with GAT). Subsequently, appropriate amount of rape seeds was sown in each pot, and after germination, the seedlings were thinned to 3 plants per pot. The pots were watered daily with suitable amount of tap water. Each pot group comprised three replicates. After 35 days, the plant height, leaf width, fresh weight, and dry weight of the rape seedlings were recorded.

RESULTS

Characterization of the adsorbent before and after thermal modification

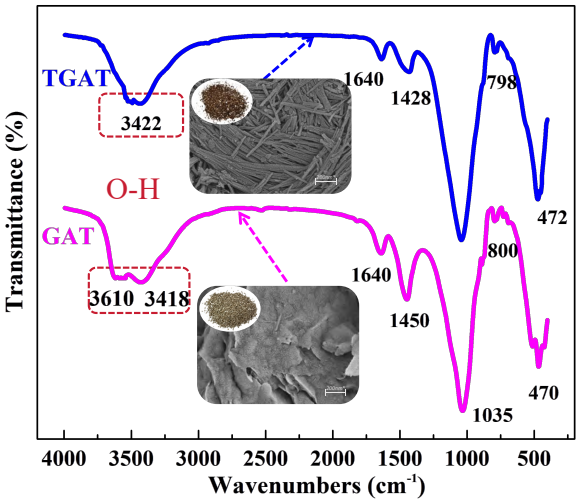

Fig. 1 FTIR and SEM spectrum of GAT and TGAT.

The FTIR spectra of the adsorbent before and after thermal modification are shown in Fig. 1. The GAT exhibited absorption peaks at 1640, 3418, and 3610 cm^{-1}, which mainly corresponded to the bending vibration peaks of physical adsorption of water in attapulgite, zeolite water, and hydroxyl stretching vibration peaks, respectively [15], and the peaks at 1450 cm^{-1} indicated the bending vibration of amorphous carbonate (CO_3^{2-}) in dolomite [16]. After thermal treatment, the strength of hydroxyl stretching vibration at 1640 cm^{-1} was weakened, the peak strength of groups associated with amorphous carbonates at 1450 cm^{-1} was reduced, and no residue of hydroxyl-related bands was observed at 3610 cm^{-1} [17]. These results showed that under high temperatures, zeolite water in the pore, coordination water molecules at the edge of the octahedron, and structural water in the middle of the octahedral layer were removed and the dolomite was decomposed. However, the vibration peaks corresponding to O—Si—O and Si—O—Si bonds at 470 and 1035 cm^{-1} were only slightly altered, indicating that the crystallinity of quartz was almost unaffected by temperature [18]. This finding is consistent with those reported in our previous studies [19]. Moreover, the color of the adsorbent changed from gray to reddish-brown after thermal treatment, which may be caused by the release of metal ions. The SEM images showed that the adsorbent presented significant rod-like structures after thermal treatment, which may be related to the reduction of the hydroxyl band and structural water [20].

Table 3 Physicochemical properties of GAT and TGAT.

Property	GAT	TGAT
BET surface area (m^2/g)	116.609	62.532
Pore volume (cm^3/g)	0.200	0.177
Total Ca (mg/g)	46.821	62.247
Total Fe (mg/g)	41.104	64.268
Total Mg (mg/g)	20.298	23.104
Total Al (mg/g)	40.472	44.639
LOI (%)	21.06	15.89
SiO_2	50.36	55.93
CaO	15.69	19.42
MgO	11.26	13.52
Al_2O_3	5.14	7.98
Fe_2O_3	4.26	6.02
Zeta (mV)	−17.324	−14.257

The physicochemical properties of GAT before and after thermal modification are shown in Table 3. The specific surface area of GAT was 116.609 m^2/g, while that of TGAT was reduced to 62.532 m^2/g, which may be predominantly attributed to the collapse of the internal structure of GAT after thermal treatment. Some studies have suggested that the enhanced pollutant adsorption performance of TGAT cannot be explained by the reaming-induced mechanism caused by dehydration [21]. The change in specific surface area and pore does not significantly affect the adsorption performance, but is mainly related to the surface properties [22]. In the present study, ICP-OES results revealed that the metal content of attapulgite increased after thermal treatment. The contents of Ca, Fe, Mg, and Al were increased from 46.821, 41.104, 20.298, and 40.472 mg/g to 62.247, 64.268, 23.104, and 44.639 mg/g, respectively. In addition, the Zeta potential of GAT was noted to be −17.324 mV, while that of TGAT increased to −14.257 mV. The decrease in the surface negative charge of the adsorbent following thermal treatment could mainly be attributed to the exposure of many positively charged metal active groups within the pores and surfaces of the octahedron and tetrahedron of the attapulgite fiber after thermal treatment [23], thereby enhancing the probability of reacting with anions in water.

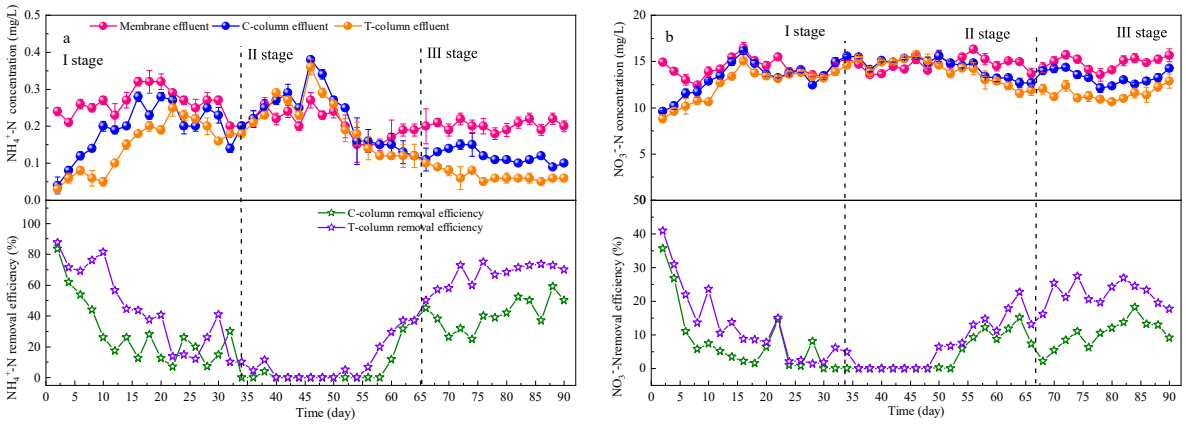

Fig. 2 Change in (a) NH_4^+-N and (b) NO_3^--N concentrations and the corresponding removal efficiencies.

Nitrogen removal effect

Fig. 2a shows the efficacy of the fixed-bed column in removing NH_4^+-N in the A/O-MBR effluent. During the operation period, the NH_4^+-N concentration in the effluent of the GAT and TGAT groups first decreased and then increased. By the end of the reactor operation, the NH_4^+-N removal efficiency of the GAT and TGAT groups reached 24.22% and 39.00%, respectively. These results indicated that TGAT exhibited better NH_4^+-N removal efficacy than GAT.

The change in the NH_4^+-N concentration in the effluent of the fixed-bed column during the entire operation period was divided into three stages: adsorption N removal stage (I stage, 0–34 days), biofilm formation stage (II stage, 35–58 days), and biological removal stage (III stage, 59–90 days). In the I stage, the removal of NH_4^+-N mainly depended on the adsorption of adsorbent, and the reactor operation tended to remain stable, with NH_4^+-N content of about 0.26 ± 0.06 mg/l in the membrane effluent. However, with the continuous adsorption and removal processes, an equilibrium state was gradually attained, and the NH_4^+-N removal efficacy began to progressively decrease, dropping to zero on day 34. The average NH_4^+-N removal efficiency of the C-column and T-column in the I stage was 29.41% and 45.36%, respectively, with the T-column exhibiting significantly enhanced NH_4^+-N removal effect than the C-column. In the II stage, with the increase in the NH_4^+-N concentration in the effluent of the fixed-bed column, the average NH_4^+-N concentration in the effluent of the C-column and T-column decreased to zero with the continuous operation of the reactor. A mature and stable biofilm was formed on the adsorbent surface, which gradually led to biological N removal. In the III stage, the biological N removal process as well as the NH_4^+-N concentration in the effluent of the C-column and T-column began to decline. At the end of the III stage, the NH_4^+-N concentrations in the effluent of the C-column and T-column were 0.11 and 0.06 mg/l, corresponding to 50.00% and 70.02% higher NH_4^+-N removal efficiency, respectively.

The nitrate N (NO_3^--N) removal efficacies of the C-column and T-column are shown in Fig. 2b. The concentration of NO_3^--N in the membrane effluent fluctuated in the range of 13.01–16.48 mg/l. Although the removal of NO_3^--N by the fixed-bed columns was insignificant, the overall trend was similar to that of NH_4^+-N removal. In other words, the NO_3^--N removal process by the fixed-bed column can also be divided into three stages. In the I stage (0–34 days), a certain amount of NO_3^--N was removed by both the C-column and T-column, with average NO_3^--N removal efficiency reaching 7.62% and 12.59%, respectively, within 34 days. With the continuous operation of the reactor (III stage, biological denitrification stage), NO_3^--N was reduced to N2 under the action of organic carbon source and denitrifying bacteria, and the NO_3^--N concentration in the effluent was further reduced. The NO_3^--N concentration in the effluent of the C-column and T-column decreased from 13.21 and 12.86 mg/l to 12.36 and 10.65 mg/l, corresponding to 12.09% and 24.25% increase in the removal efficiency, respectively.

The changes in the TN concentration in the effluent of the C-column and T-column are shown in Fig. 3a. The TN concentration in the membrane effluent fluctuated between 14.09 and 17.55 mg/l, and the TN concentration in the effluent of the two groups of fixed-bed columns first increased and then decreased. During the initial stage of operation, the T-column presented better TN removal effect than the C-column. In the I stage, the average TN removal efficiencies of the T-column and C-column were 19.36% and 11.16%, respectively. In the II stage involving biofilm growth, the TN concentration in the effluent of the C-column and T-column was higher, similar to the changes in the NH_4^+-N and NO_3^--N concentrations, and the average TN concentration increased from 15.77 to 16.79 and 16.57 mg/l, respectively. In the III stage, the TN con-

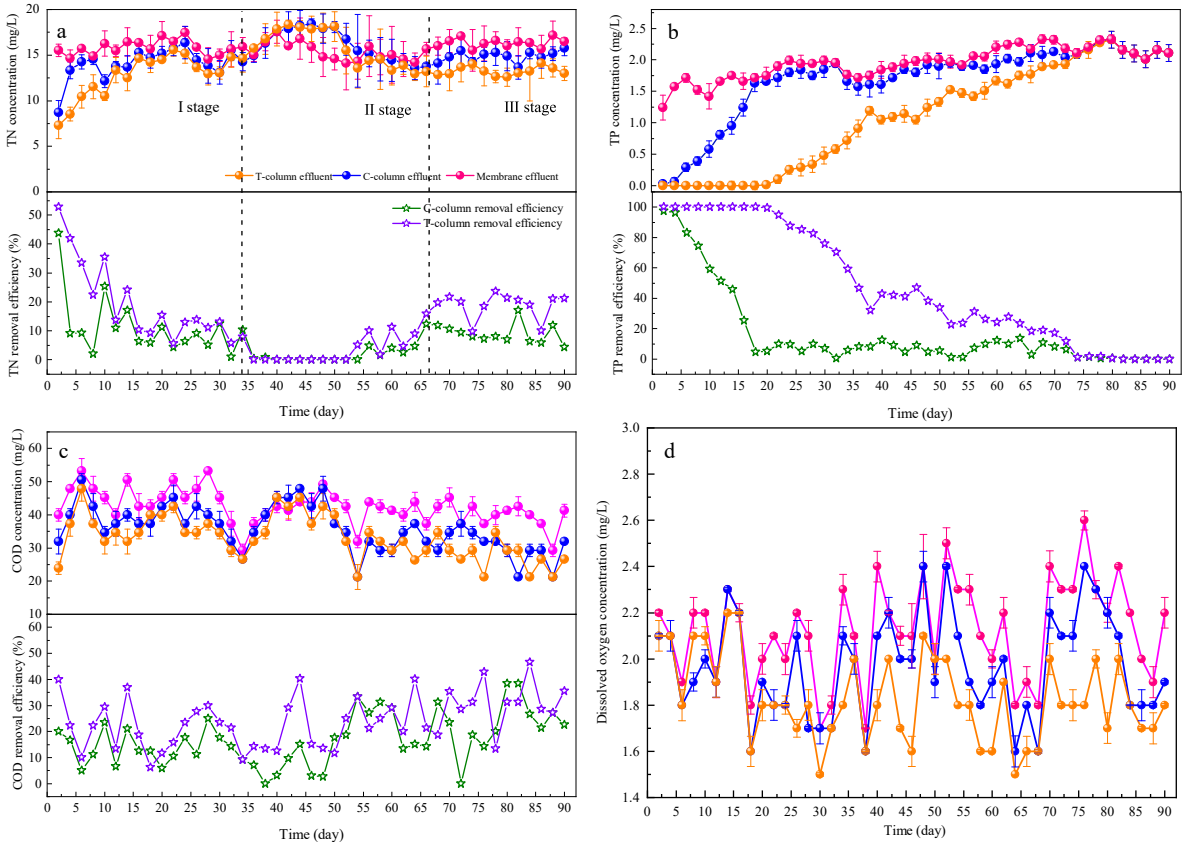

Fig. 3 Changes in the (a) TN (b) TP (c) COD and (d) dissolved oxygen concentrations and the corresponding removal efficiencies.

centration in the effluent gradually decreased under the action of denitrifying microorganisms, reaching 15.79 and 12.99 mg/l in the C-column and T-column, respectively, after 90 days of operation.

Phosphorus removal performance

During stable operation, the TP concentration in the membrane effluent fluctuated between 1.24 and 2.33 mg/l (Fig. 3b). The TP concentration in the effluent of the T-column was undetectable in the initial 18 days, and then gradually increased, reaching the breakthrough concentration of 0.5 mg/l on day 30. In the C-column, the TP concentration in the effluent increased from the initial 0.03 mg/l to the breakthrough concentration of 0.5 mg/l on day 9. With continued operation of the reactor, the TP concentration in the effluent of the C-column and T-column reached the depletion concentration on day 18 ($C_t/C_0 = 0.9$) and day 72, respectively. The average TP removal efficiencies of the C-column and T-column were 18.44% and 53.20%, respectively, with the T-column exhibiting 100% removal efficiency in the first 18 days. These results revealed that the fixed-bed column could effectively reduce the P concentration in the MBR effluent, thereby achieving substantial P removal.

COD removal effect

In the A/O-MBR system, the majority of organic substances are intercepted and eliminated through membrane filtration of the system effluent. The COD concentration of the membrane effluent fluctuates within the range of 29.27 mg/l to 53.23 mg/l (Fig. 3c).

Following the treatment of the membrane effluent by fixed-bed adsorption, the COD concentration of the final effluent exhibits a trend of initial increase followed by subsequent decrease-a pattern analogous to the removal profile of TN, while the overall variation remains negligible. Over the 90 days operational period, the average effluent COD concentrations of the two fixed-bed columns were 35.33 mg/l and 32.03 mg/l, corresponding to average removal efficiencies of 16.40% and 24.19%, respectively.

Variations in dissolved oxygen

This study analyzed the variations in dissolved oxygen (DO) concentrations of MBR effluent and effluents from two fixed-bed columns (Fig. 3d). During the 90-day operation, the DO concentration of MBR effluent fluctuated between 1.7–2.6 mg/l, with an average value of 2.1 mg/l. Both fixed-bed columns significantly reduced effluent DO levels. The C-column effluent

DO ranged from 1.6–2.4 mg/l (average: 1.95 mg/l), while the T-column effluent DO stabilized at 1.5–2.2 mg/l, with a lower average of 1.85 mg/l and a minimum of 1.5 mg/l, exhibiting a considerably higher DO reduction magnitude. The DO reduction extent of both columns increased with operation time. After 34 days of operation, the T-column showed a more distinct DO decrease and sustained lower effluent DO concentrations than the C-column, indicating dynamic variations in internal DO consumption within the fixed-bed system during long-term operation.

Feasibility of TGAT as a slow-release fertilizer after wastewater treatment

Following its application in wastewater treatment, the used TGAT adsorbent was employed as a fertilizer in rape pots to examine its potential as a substitute for chemical fertilizers. After a 6-week period of cultivation, the plant height, leaf width, fresh weight, and dry weight of rape seedlings in the TGAT group increased by 75.13%, 84.64%, 202.48%, and 204.13%, respectively. In contrast, only moderate growth promotion effects were observed in the control (GAT) group, with the plant height, leaf width, fresh weight, and dry weight increasing by 13.80%, 25.58%, 89.45% and 29.88%, respectively.

DISCUSSION

The NH_4^+-N removal process generally presents a trend of an initial increase, a decrease, and a subsequent increase in the NH_4^+-N content. In the initial stage, physical adsorption is the predominant mechanism. Previous studies have shown that the NH_4^+-N removal performance of attapulgite was enhanced after thermal treatment, mainly because the ammonia ion, which has a considerably smaller radius (about 1.48 Å) than the phosphoric acid ion (2.38 Å), can enter the pore faster to achieve physical adsorption of NH_4^+-N [24]. Membrane filtration is an effective method for removing microorganisms and suspended particulate matter in wastewater. However, the effluent may still contain negligible quantity of free microbial cells that can easily adhere to the surface of the porous adsorbent carrier and gradually proliferate by utilizing the limited amount of organic matter in the effluent as carbon source to form biofilm. Natural minerals are excellent microbial attachment carriers with high compressive strength and abundant open pores and rough surfaces, which are conducive to the fixation and attachment of microorganisms [24]. Zeng et al [25] prepared a composite filter filler comprising natural materials such as zeolite, quartz sand, and ceramic particles, and found that the filler along with autotrophic denitrifying bacteria, exhibited average NH_4^+-N, TN, and TP removal efficiencies of 66.4%, 58.1%, and 85%, respectively. Bao et al [26] used a composite material (FCM) comprising palygorskite clay, goethite, and sawdust as filler for the biological aerated filter, which effectively removed N and P from domestic wastewater. When compared with commercial ceramide, FCM biofilm presented faster growth rate, higher abundance, and greater diversity of denitrifying microorganisms.

In the present study, denitrifying microorganisms in the A/O-MBR system entered the fixed-bed column with the membrane effluent and attached and grew on the adsorbent surface and pores in the fixed-bed column, forming a biofilm. During the growth of the biofilm, the microbial metabolism was vigorous, with simultaneous death of some microorganisms, and the NH_4^+-N removal by the fixed-bed column significantly decreased. However, with the continued operation of the reactor, a mature and stable biofilm was formed on the surface of the adsorbent, gradually resulting in biological N removal. During this stage, the denitrifying microorganisms converted NH_4^+-N into nitrate, facilitating subsequent removal of N. Thus, biological process plays an essential role in removing NH_4^+-N during the late stage of reactor operation.

The presence of a large number of pore structures and cavities in the adsorbent at the initial stage of operation facilitated the removal of a part of NO_3^--N via physical adsorption. The NO_3^--N removal efficiency of TGAT was slightly better than that of GAT, which could mainly be attributed to the absorption of a large number of positively charged metal ion groups on the internal pores and surface of attapulgite after thermal treatment. This resulted in an increase in the surface positive charge (Zeta potential increased from −17.324 to −14.257 mV) and electrostatic attraction between attapulgite and NO_3^--N anion, which further improved the NO_3^--N removal ability [27]. However, with the continued operation of the reactor, no significant difference was noted in the NO_3^--N concentration in the effluent of the two groups of fixed-bed columns. In the II stage, the NO_3^--N concentration in the effluent of the fixed-bed column was higher than that in the membrane effluent mainly owing to nitrification resulting from the autolysis of microorganisms in the biofilm. Under the combined action of Ammonia Oxidizing Bacteria (AOB) and Nitrite Oxidizing Bacteria (NOB), NH_4^+-N is removed and NO_3^--N is produced [28, 29].

In general, the N removal efficiency of the fixed-bed columns was limited during reactor operation. In the initial stage of operation, N removal was achieved via physical adsorption and the N removal efficiency of the fixed-bed columns first increased and then decreased. The subsequent microbial attachment, growth, and proliferation on the adsorbent surface or in the pore resulted in vigorous microbial metabolism and steady biofilm formation, thereby leading to progressive biological N removal. Consequently, the TN concentration in the effluent decreased, and the TN removal rate increased. At the end of the operation, the average TN removal efficiencies of the C-column and T-column were 8.18% and 16.67%, respectively. The re-

moval of TN was predominantly attributed to biological N removal, with minimal contribution from adsorption and N elimination involving adsorbents. Some studies have found that the performance of denitrifying microorganisms can be synergistically enhanced through interface interaction between clay minerals and microorganisms, improving the electron exchange capacity and transfer rate during denitrification and promoting microbial metabolic activities to increase the efficiency of biological N removal [30]. Microbial metabolism can stimulate the release of cations from clay minerals, form cation bridges, promote the adsorption and aggregation of clay minerals to denitrifying microorganisms, and form biofilm conducive to microbial growth [31]. Clay minerals can increase the secretion of bioelectronic conductive substances and facilitate extracellular electron transfer, which is beneficial to improving the denitrification rate between the N removal systems [32]. Besides, clay minerals can increase the activity of key enzymes during denitrification as well as enhance effective electron transfer during microbial metabolic activities, thus improving the N removal efficiency [33].

In the present study, TGAT exhibited remarkable ability to remove P from wastewater, achieved through chemical surface precipitation of metal ions on the TGAT surface and phosphoric acid in wastewater [34]. When compared with the GAT, TGAT showed superior ability to remove P from low-concentration P-containing wastewater, because the presence of a certain amount of metal cations (e.g., Mg^{2+}, Ca^{2+}, and Fe^{3+}) in the membrane effluent strengthened the electrostatic adsorption removal of phosphate anion by TGAT.

During the initial phase of operation, COD attenuation is primarily driven by physical adsorption within the mesoporous structure of attapulgite. Importantly, this pore-based adsorption mechanism exerts negligible influence on the P removal capacity of TGAT. As biofilm development progresses on the attapulgite surface, microbial activity becomes increasingly dominant: heterotrophic denitrifying bacteria mediate COD consumption through denitrification—simultaneously generating energy that supports the growth and metabolic activity of coexisting microorganisms.

Biofilm maturation on thermal attapulgite carriers governed the effluent DO profile and pollutant removal of the T-column. Stage I featured immature biofilms and low microbial activity, causing limited DO consumption and slightly reduced effluent DO. The porous, surface-modified structure of thermal attapulgite subsequently facilitated microbial colonization and biofilm maturation, and intensified aerobic respiration depleted in-column DO, establishing a stable anoxic/micro-aerobic environment with T-column effluent DO of 1.5–2.2 mg/l. This microenvironment supported denitrifier growth and enhanced biological denitrification using residual nitrate in MBR effluent, improving systemic N removal. The T-column removed N via early pore adsorption and later biological processes, and N adsorption exerted negligible effects on phosphate removal [35]. Biofilm-driven interfacial mass transfer enabled reactions between sewage phosphoric acid and attapulgite metal ions, so biofilm growth barely affected TP removal [36]. During Stage II and Stage III, the T-column and C-column obtained average TP removal efficiencies of 34.98% and 18.18%, respectively, and the gradual decay in TP removal was attributed to progressive adsorption site consumption and saturation. Overall, TGAT achieved N removal mainly through biological pathways, while P removal relied primarily on chemical precipitation between wastewater phosphoric acid and material metal ions (Fig. 4).

Clay minerals are rich in trace elements required for plant growth, which can effectively improve crop quality and yield [37]. Moreover, the abundant internal nanopores can ensure excellent water and fertility retention as well as adsorb chemical substances in soil that are not conducive to plant growth, thus reducing plant growth resistance. Rape is a calcium-loving plant, and application of TGAT to soil can enhance calcium availability, thereby promoting the growth of rape [38]. In the present study, SEM-energy-dispersive

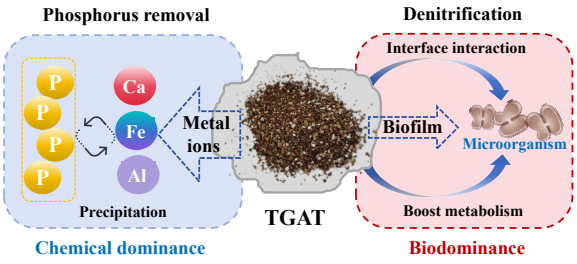

Fig. 4 Mechanism of nitrogen and phosphorus removal by TGAT.

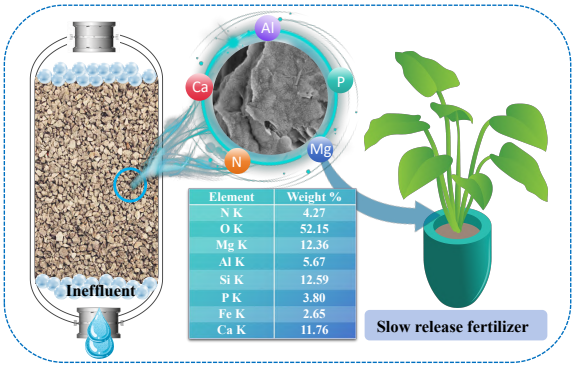

Fig. 5 TGAT after wastewater treatment is used as a slow-release fertilizer for plants.

X-ray spectroscopy (EDS) images of the adsorbed material (Fig. 5) revealed no apparent tight rod-like structure on the TGAT surface, which could be attributed to the formation of biofilm on the adsorbent surface. EDS elemental analysis results showed that the main components of TGAT were O, Si, Mg, Ca, Al, N, P, and Fe, which do not produce any detrimental effects on soil and crops, indicating that TGAT can be used as a slow-release fertilizer. After wastewater treatment, TGAT was noted to be rich in N, P, and trace metal elements that can promote plant growth. Besides, TGAT can remove N and P pollutants from wastewater mainly via surface precipitation and formation of N-containing products. Some studies have suggested that P in the Ca-P binding state is the primary source of P in soil available to crops, which can exert a positive effect on crop growth [23]. These sediments usually present low solubility, which not only facilitates slow release of nutrients, but also prevents entry of pollutants into the surface water, causing agricultural non-point source pollution [39, 40].

CONCLUSION

In this study, TGAT prepared by thermal treatment of GAT showed excellent N and P removal from A/O-MBR effluent. To verify the practical applications of TGAT, an A/O-MBR fixed-bed column reactor was constructed and operated for 90 days. The results revealed that TGAT could simultaneously remove N and P pollutants in wastewater, showing 16.67%, 70.02%, 24.25%, and 53.20% higher TN, NH_4^+-N, NO_3^--N, and TP removal efficiencies, respectively, when compared with those exhibited by GAT (8.18%, 50.00%, 12.09%, and 18.44%, respectively). The removal of N-containing pollutants by TGAT was accomplished in three stages: adsorption (I stage), biofilm formation (II stage), and biological removal (III stage), with biological removal being the major step. The P-containing pollutants were primarily removed by TGAT via surface precipitation. The SEM-EDS results showed that the main components of the adsorbed TGAT included O, Ca, Si, Mg, Al, P, N, Fe, and K, which were nontoxic to soil and crop growth. The pot experiments indicated that TGAT could promote the development of rape, increasing the plant height, leaf width, fresh weight, and dry weight. Therefore, TGAT was considered as a promising filler for treating N and P pollutants in wastewater, as well as for its subsequent reuse as a slow-release fertilizer in agricultural soils.

Acknowledgements: This work was supported by the Jiangsu Province university philosophy and social science research project under Grant 2022SJSZ0964; Jiangsu Province Education Science Planning Project under Grant B-b/2024/02/14; and Basic Application Research Project of Lianyungang Technical College under Grant XYB202425.

REFERENCES

1. Miwa T, Nagatsuma S, Hirakata Y, Nagai M, Ikarashi TY, Takimoto Y, Watari T, Yamaguchi T, et al (2024) Combination of a membrane bioreactor with a rotating biological contactor holding several diverse metazoans can reduce excess sludge with fouling mitigation. *Water Res* **266**, 122352.
2. Lee G, Modarresi S, Benjamin MM (2019) Efficient phosphorus removal from MBR effluent with heated aluminum oxide particles (HAOPs). *Water Res* **159**, 274–282.
3. Zhou Y, Li X (2022) Effect of addition sites on bioaugmentation of tea polyphenols-NZVI/PE composite packing: Nitrogen removal efficiency and service life. *Chemosphere* **290**, 133258.
4. Yuan LM, Zhang CY, Xu JY, Chu JS, Wang BB, Wu QW, Liu JT (2015) Performance of an innovative step-feed An-M(A/O)-MBR process for nutrients removal. *Desalin Water Trea* **55**, 2728–2733.
5. Omwene PI, Kobya M (2018) Treatment of domestic wastewater phosphate by electrocoagulation using Fe and Al electrodes: A comparative study. *Process Saf Environ Prot* **116**, 34–51.
6. Gizaw A, Zewge F, Kumar A, Mekonnen A, Tesfaye M (2021) A comprehensive review on nitrate and phosphate removal and recovery from aqueous solutions by adsorption. *J Water Supply Res Technol AQUA* **70**, 921–947.
7. Jung KW, Jeong TU, Choi JW, Ahn KH, Lee SH (2017) Adsorption of phosphate from aqueous solution using electrochemically modified biochar calcium-alginate beads: Batch and fixed-bed column performance. *Bioresour Technol* **244**, 23–32.
8. Zamparas M, Kapsalis V, Kanteraki AE, Vardoulakis E, Kalavrouziotis IK (2018) Novel composite materials as P-adsorption agents and their potential application as fertilizers. *Global NEST J* **21**, 48–57.
9. Liu B, Liu Z, Wu H, Pan S, Sun Y, Xu Y (2021) Insight into simultaneous selective removal of nitrogen and phosphorus species by lanthanum-modified porous polymer: Performance, mechanism and application. *Chem Eng J* **415**.
10. Yu C (2022) Recovery of NH_4^+-N and PO_4^{3-}-P from urine using sludge-derived biochar as a fertilizer: Performance and mechanism. *RSC Adv* **12**, 4224–4233.
11. Huang YX, Liu MJ, Chen S, Jasmi II, Tang Y, Lin S (2019) Enhanced adsorption and slow release of phosphate by dolomite-alginate composite beads as potential fertilizer. *Water Environ Res* **91**, 797–804.
12. Zhao Y, Yang Y, Yang S, Wang Q, Feng C, Zhang Z (2013) Adsorption of high ammonium nitrogen from wastewater using a novel ceramic adsorbent and the evaluation of the ammonium-adsorbed-ceramic as fertilizer. *J Colloid Interface Sci* **393**, 264–270.
13. Sornhiran N, Tuntrachanida J, Malachey P, Thongtuk P, Wisawapipat W, Aramrak S, Prakongkep N (2021) Aluminum- and iron-engineered biochar from sugarcane filter cake as phosphorus adsorbents and fertilizers. *ScienceAsia* **47**, 220–227.
14. Kong L, Tian Y, Li N, Liu Y, Zhang J, Zhang J, Zuo W (2018) Highly-effective phosphate removal from aqueous solutions by calcined nano-porous palygorskite matrix with embedded lanthanum hydroxide. *Appl Clay Sci*

162, 507–517.
15. Hei S, Xu H, Liu Y, Liu B, Zhang S, Zhu X, Lin W, Chen L, et al (2022) Redox environment inducing strategy for enhancing biological phosphorus removal in a full-scale municipal wastewater treatment plant. *J Cleaner Production* **376**.
16. Huang W, Zhang Y, Li D (2017) Adsorptive removal of phosphate from water using mesoporous materials: A review. *J Environ Manage* **193**, 470–482.
17. Lv N, Li X, Qi X, Ren Y (2022) Calcium-modified granular attapulgite removed phosphorus from synthetic wastewater containing low-strength phosphorus. *Chemosphere* **296**, 133898.
18. Kumar M, Badruzzaman M, Adham S, Oppenheimer J (2007) Beneficial phosphate recovery from reverse osmosis (RO) concentrate of an integrated membrane system using polymeric ligand exchanger (PLE). *Water Res* **41**, 2211–2219.
19. Lv N, Li X (2022) Phosphorus removal from wastewater using Ca-modified attapulgite: Fixed-bed column performance and breakthrough curves analysis. *J Environ Manage* **328**, 116905.
20. Gan F, Zhou J, Wang H, Du C, Chen X (2009) Removal of phosphate from aqueous solution by thermally treated natural palygorskite. *Water Res* **43**, 2907–2915.
21. Xie JJ, Chen THH, Qing CS, Chen D, Zhu CZ, Wang JY, Zhan XM (2013) Adsorption of phosphate from aqueous solutions by thermally modified palygorskite. *Environ Eng Manag J* **12**, 1393–1399.
22. Piroddi C, Teixeira H, Lynam CP, Smith C, Alvarez MC, Mazik K, Andonegi E, Churilova T, et al (2015) Using ecological models to assess ecosystem status in support of the European Marine Strategy Framework Directive. *Ecol Indicators* **58**, 175–191.
23. Mitrogiannis D, Psychoyou M, Baziotis I, Inglezakis VJ, Koukouzas N, Tsoukalas N, Palles D, Kamitsos E, et al (2017) Removal of phosphate from aqueous solutions by adsorption onto $Ca(OH)_2$ treated natural clinoptilolite. *Chem Eng J* **320**, 510–522.
24. Zhang Y, Lu C, Chen Z, Song Y, Li H, Han Y, Hou Y, Guo J (2022) Multifaceted synergistic electron transfer mechanism for enhancing denitrification by clay minerals. *Sci Total Environ* **812**, 152222.
25. Zeng Y, Xu W, Wang H, Zhao D, Ding H (2022) Nitrogen and phosphorus removal efficiency and denitrification kinetics of different substrates in constructed wetland. *Water* **14**, 1757.
26. Bao T, Damtie MM, Yu ZM, Liu Y, Jin J, Wu K, Deng CX, Wei W, et al (2019) Green synthesis of Fe_3O_4@carbon filter media for simultaneous phosphate recovery and nitrogen removal from domestic wastewater in biological aerated filters. *ACS Sust Chem Eng* **7**, 16698–16709.
27. Hu A, Ren G, Che J, Guo Y, Ye J, Zhou S (2020) Phosphate recovery with granular acid-activated neutralized red mud: Fixed-bed column performance and breakthrough curve modelling. *J Environ Sci* **90**, 78–86.
28. Gao F, Zhang H, Yang F, Qiang H, Li H, Zhang R (2013) Study of an innovative anaerobic (A)/oxic (O)/anaerobic (A) bioreactor based on denitrification–anammox technology treating low C/N municipal sewage. *Chem Eng J* **232**, 65–73.
29. Adoonsook D, Chia-Yuan C, Wongrueng A, Pumas C (2019) A simple way to improve a conventional A/O-MBR for high simultaneous carbon and nutrient removal from synthetic municipal wastewater. *PLoS One* **14**, e0214976.
30. Li GL, Zhou CH, Fiore S, Yu WH (2019) Interactions between microorganisms and clay minerals: New insights and broader applications. *Appl Clay Sci* **177**, 91–113.
31. Dong H, Jaisi DP, Kim J, Zhang G (2009) Microbe-clay mineral interactions. *Am Mineral* **94**, 1505–1519.
32. Yang X, He Q, Guo F, Sun X, Zhang J, Chen M, Vymazal J, Chen Y (2020) Nanoplastics disturb nitrogen removal in constructed wetlands: Responses of microbes and macrophytes. *Environ Sci Technol* **54**, 14007–14016.
33. Deng C, Xue J, Wu Y (2022) Using magnetite/zirconium-comodified attapulgite as a novel phosphorus (P) sorbent for the efficient removal of P and the adsorption mechanism allowing this effect. *Appl Water Sci* **13**, 12.
34. Yang X, Chen J, Wu X, Zhu G (2024) Toward a better understanding of polymeric aluminum-modified attapulgite for the efficient removal of low phosphorus concentration. *Water Environ Res* **96**, e11122.
35. Dou H, Tang N, Wang Y, Su J, Yang Q, Yang Z (2024) The aerobic biofilm on naphthalene as the carbon source: Growth, biodegradability, and mass transfer-diffusion kinetics. *Process Biochem* **139**, 165–174.
36. Mohammadi N, Shariatmadari H (2020) Effect of magnesium silicate nanocomposites coating of phosphate fertilizer on the availability and plant uptake of phosphorus. *Commun Soil Sci Plant Anal* **51**, 2581–2591.
37. Hong SH, Ndingwan AM, Yoo SC, Lee CG, Park SJ (2020) Use of calcined sepiolite in removing phosphate from water and returning phosphate to soil as phosphorus fertilizer. *J Environ Manage* **270**, 110817.
38. Kenawy E-R, Elnaby HH, Azaam MM (2023) Synthesis of superabsorbent composite based on chitosan-g-poly(acrylamide)/attapulgite. *Polym Bull* **81**, 3527–3543.
39. Hylander L, Simán G (2001) Plant availability of phosphorus sorbed to potential wastewater treatment materials. *Biol Fertility Soils* **34**, 42–48.
40. Kuang X, Li J, Ouyang Z, Huang H, Chen J, Chen X, Li L (2024) Ca–Mg modified attapulgite for phosphate removal and its potential as phosphate-based fertilizer. *J Environ Manage* **357**, 120727.